Heliyon 7 (2021) e06373

Contents lists available at ScienceDirect

Heliyon

journal homepage: www.cell.com/heliyon

Research article

A novel quadband ultra miniaturized planar antenna with metallic vias and defected ground structure for portable devices

Pierre Moukala Mpele [a,*], Franck Moukanda Mbango [b], Dominic B.O. Konditi [c], Fabien Ndagijimana [d]

[a] Department of Electrical Engineering, Pan African University Institute of Basic Sciences Technology and Innovation (PAUSTI), Nairobi, Kenya
[b] Faculty of Sciences and Techniques, Electrical and Electronics Engineering Laboratory, Marien Ngouabi University, B.P 69, Brazzaville, Congo
[c] School of Electrical and Electronics Engineering, Technical University of Kenya (TUK), Nairobi, Kenya
[d] Electrical Engineering Department, Univ. Grenoble Alpes, CNRS, G2ELab, 151 Rue de la Papeterie, F-38400, Saint-Martin d'Hères, France

ARTICLE INFO

Keywords:
Miniature antenna
Heart-shaped antenna
Monopole antenna
Multiband
Mobile communication
Portable devices
Wireless communication systems

ABSTRACT

A novel heart-shaped monopole antenna used in wireless portable communication devices is proposed and discussed in this paper. The antenna has a radiant patch surface area of 28.504 mm^2, the physical size of 15 × 12.5 × 1 mm^3, and electrical dimensions of $0.095\lambda_0 \times 0.079\lambda_0 \times 0.006\lambda_0$, where λ_0 denotes the wavelength of the free space at 1.89 GHz. Its prototype is printed on FR4 HTG-175, having a permittivity of 4.2 and a loss tangent of 0.019 at 1 GHz. The partial ground plane and two metallic vias connecting two open-ended branches of the slitted radiating patch to a parasitic conductor element results in about 98% miniaturization of the active patch area, as compared to the conventional antenna. The proposed antenna exhibits nearly an omnidirectional pattern in the elevation plane with a maximum radiation efficiency of 82.78% at 3.99 GHz, while a peak gain of 4.7 dBi is obtained at 6.5 GHz. The measured -6 dB impedance bandwidths demonstrate that the proposed quadband antenna operates in all the frequency bands of mobile telecommunication standards (2G/3G/4G/5G) and other applications, including WLAN, WiMAX, ISM, meteorological services, IEEE 802.11y, and C-band satellite communications. This antenna is easy to manufacture and can be used in most portable devices as a compact internal antenna. After simulating the modeled antenna using HFSS, a prototype was experimentally tested, and the measured results were compared with the data obtained by simulation. The parameters analyzed are return loss, bandwidth, and gain on all frequency bands. The fabricated prototype guarantees a minimum -10 dB bandwidth of 110 MHz and a maximum return loss of -12.2 dB, despite its low radiation efficiency of 21.43 % in the lower band dedicated to GSM applications. Furthermore, the proposed antenna operates as a narrowband and wideband.

1. Introduction

The commercial mobile communications industry has been the catalyst for the recent explosive growth in antenna design needs [1]. These technologies include the mobile telecommunication standards (GSM, DCS, PCS UMTS, LTE, 5G NR) and other modern wireless applications (WLAN, WiMAX, GPS, and so forth), which need to coexist as one in a single portable device. Multiple antennas can be used to cover different frequency bands dedicated to each wireless application. However, this results into a problem of mutual coupling or isolation [2, 3] in addition to the challenge of accommodating several internal antennas into limited space on mobile terminals [4]. Besides, a broadband antenna, covering a wide frequency range to accommodate different wireless applications in a single band, may suffer from interference problem. To address this, antennas with the capability of operating in several frequency bands while being small in size is a vital issue in wireless communications [5]. Owing to their attractive features of low cost, lightweight, small size, ease of fabrication, and wide bandwidth, planar monopole antennas are among the preferred technologies for meeting the mobile terminals' antenna requirements [6]. They are mostly designed using either microstrip feedline [7, 8] or grounded/ungrounded coplanar waveguide feed [9, 10, 11].

For mobile communication applications, the wireless terminals, such as cell phones, portable access points, laptops, and so on, are usually with

* Corresponding author.
E-mail address: pm.mpele@gmail.com (P. Moukala Mpele).

https://doi.org/10.1016/j.heliyon.2021.e06373
Received 29 December 2020; Received in revised form 15 January 2021; Accepted 22 February 2021

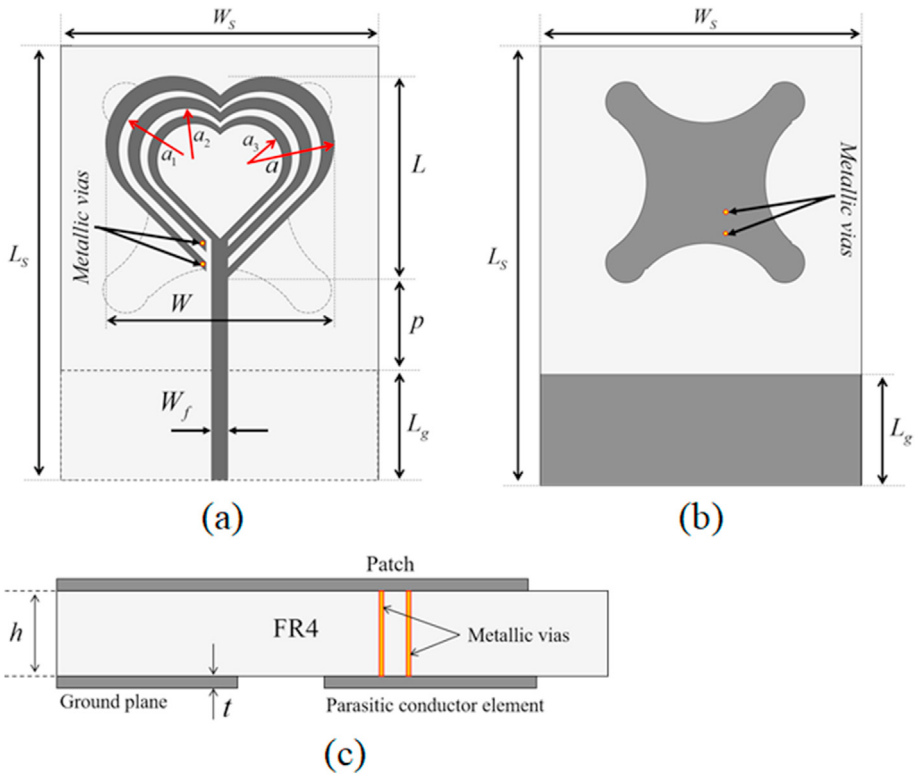

Figure 1. Antenna geometry configuration: (a) front view, (b) back view, (c) side view.

Table 1. Antenna design parameters.

Design parameter	Value (mm)
L_S	15
W_S	12.5
L	6.242
W	6.828
a	2
a_1	1.67
a_2	1.25
a_3	1
p	4.422
h	1
t	0.035
L_g	3
W_f	0.5

small volumes. The antenna structures dedicated to being mounted inside such terminals must be designed with small volumetric size, specific shapes, and areas [12]. Several promising techniques have been reported in the literature meant to reduce the microstrip antenna's size [13, 14, 15]. These techniques include the defected ground structure [16, 17, 18] approach, which is also used for antenna performance enhancement [19], high permittivity material loading [13], slots or slits loading, metamaterials [20, 21], shorting pins between the patch and the ground plane [22], use of partially shorted patch [23]. By exploiting each technique's benefits, some of the aforementioned have been combined [24] to meet some design requirements. For instance, the authors in [25] and in [26] achieved multiband and antenna size reduction using the defected ground structure (DGS) and slots techniques. A similar approach was used to design a small antenna for 2G, 3G, LTE, WLAN, and WiMAX applications in [27]. Recently, an antenna covering 2G, 3G, 4G, 5G, and WLAN applications has been proposed in [28].

Achieving miniaturization, along with good antenna performance, remains a real challenge [29, 30] in designing internal antennas with a simple structure [31] for multiband applications. The electromagnetic performances are significantly affected by the antenna geometry [32], the feeding technique [33], and the substrate material on which the antenna is printed [6].

From the literature, most of the proposed antennas dedicated to mobile devices and covering the 2G, 3G, 4G, 5G along with other wireless applications simultaneously, are metal-frame based structures, MIMO or planar monopole configurations with large size. In contrast, the other design configurations cover only a limited number of mobile telecommunication standards. In [34], a compact, multiband, uniplanar monopole antenna covering the GSM, UMTS, WLAN, WiMAX, and LTE bands was proposed. However, it requires an extensive system board with an overall size of 110 × 50 × 0.8 mm^3, limiting its applications in some handheld devices. A compact multiband antenna for mobile terminal applications for GSM, DCS, PCS, UMTS, and LTE was presented in [35] and also in [36] with a footprint of 60 × 115 mm^2 and 75 × 120 mm^2, respectively. Another nona-band narrow-frame antenna design configuration for mobile phone applications was proposed in [37]. The antenna covers the 2G, 3G, 4G, and 5G applications, but has a large volumetric size of 80 × 140 × 0.8 mm^3 using FR4 substrate. A hepta-band metal--frame antenna for LTE/WWAN full-screen smartphone was recently proposed and presented in [38]. Like the aforementioned design structures, the antenna has an overall size of 50 mm × 70 mm × 6mm while being designed on FR4 substrate with a footprint of 154 mm × 72 mm. This makes it difficult to integrate within small portable communication devices. In [39], a design of an internal compact printed loop antenna is presented for WWAN/WLAN/ISM/LTE smartphone applications. The structure exhibits good electromagnetic performance, but its large dimension of 120 × 60 × 1.6 mm^3 does not facilitate its applications in many wireless portable devices.

Trying to find one solution among several researchers, a miniaturized quadband heart-shaped planar monopole antenna (QHPMA) is proposed and discussed in this paper. This antenna is modeled and manufactured

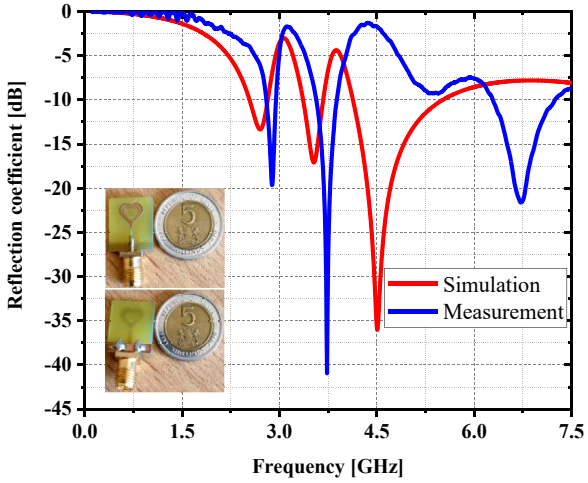

Figure 2. Simulated and measured reflection coefficients.

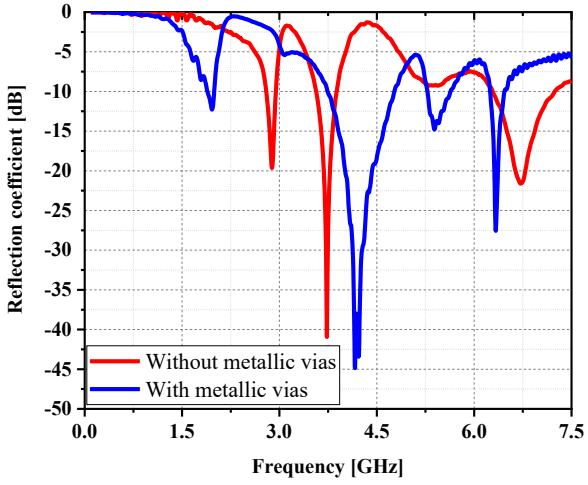

Figure 3. Measured reflection coefficient comparison.

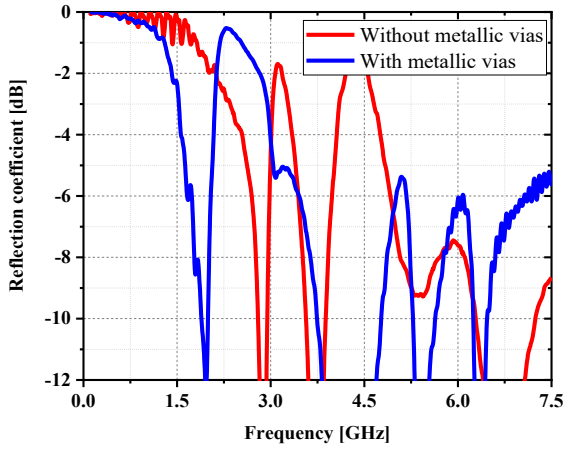

Figure 4. Zoom of the measured reflection coefficient comparison.

from the combination of the DGS, and the metallic vias that connect the parasitic conductor element placed on the bottom of the insulator material to the slitted radiating patch. This downsized antenna has been tested to demonstrate its ease of operating as a wide and narrowband device. The proposed antenna covers all cellular networks, namely the

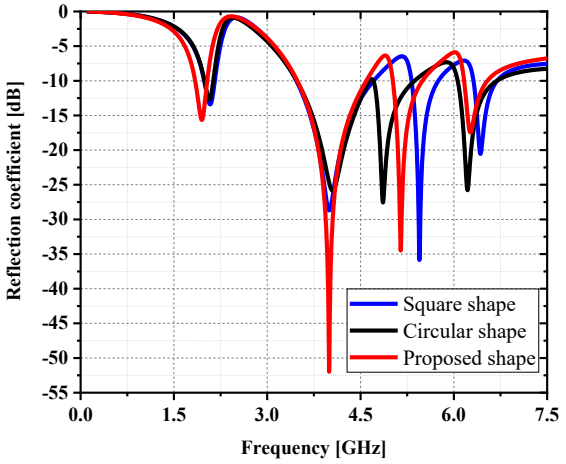

Figure 5. Impact of the parasitic element's shape.

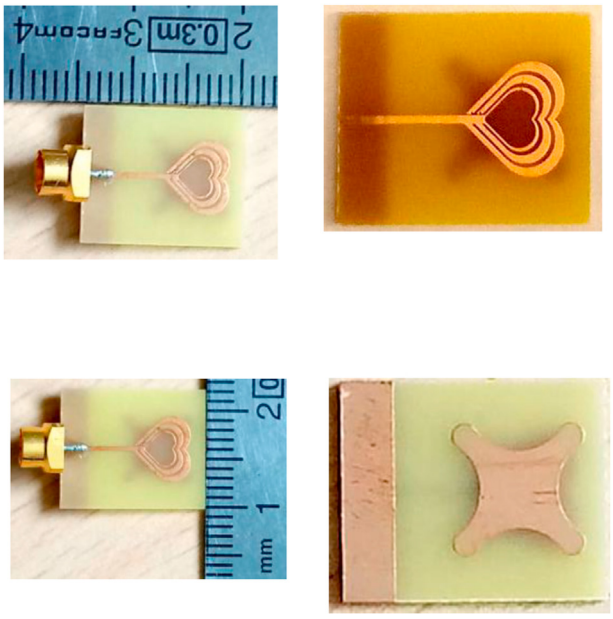

Figure 6. Photograph of the fabricated antenna: top and bottom views.

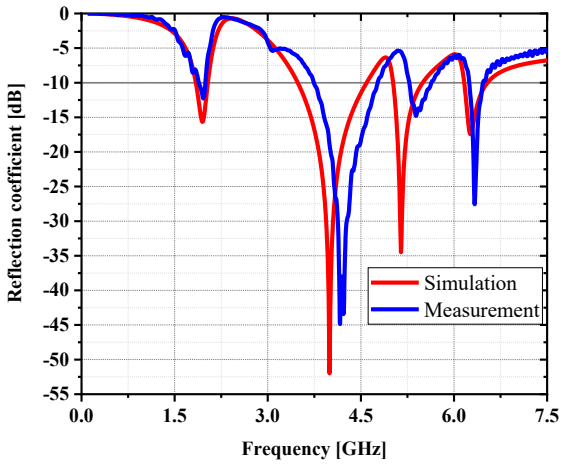

Figure 7. Simulated and measured reflection coefficients of the QHPMA.

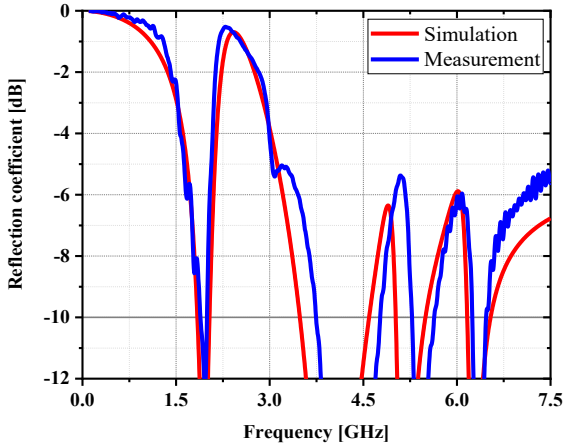

Figure 8. Zoom of the simulated and measured reflection coefficients of the QHPMA.

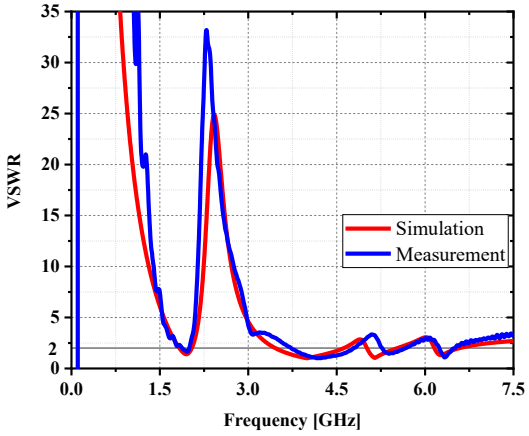

Figure 9. Simulated and measured VSWR.

second generation (2G), the third-generation (3G), the fourth generation (4G), and the fifth-generation (5G). Also, other and essential standards such as Wireless Local Area Network (WLAN), Worldwide Interoperability for Microwave Access (WiMAX), Industrial, Scientific and Medical (ISM) frequency band, and C-band satellites communications band are covered by this proposed antenna.

2. Quad-band antenna design

Figure 1 illustrates the proposed QHPMA geometry's view: the front view, the back view, and the side view. The top surface consists of two circular parts with a radius of 2 mm, merged to a 45° rotated square leading to the heart-shaped radiating patch. Two metallic vias are connected to a parasitic conductor element, placed on the insulator's bottom. The use of parasitic elements helps enhance bandwidth or create multi-band behavior [40]. In contrast, the radiating part is on the insulator's top to improve the device's return loss and create a fourth band whereas retrieving the 2G tape. A microstrip feed line is used, and the antenna is printed on an FR-4 HTG-175 which has 4.2 as a relative permittivity and 0.019 as loss tangent, determined at 1 GHz. Both values are frequency dependent and their accuracy depends on the extraction method [41, 42]. This insulator has a thickness of 1 mm. All the optimized design parameters of the proposed antenna are listed in Table 1.

The compact miniaturized heart-shaped planar monopole antenna has been achieved in three main steps:

Table 2. Wireless applications covered by the proposed antenna.

$\|S11\| \leq$ -6 dB		
Band	Bandwidth (GHz)	Applications
Band I	1.66–2.04	• GSM1800 (1710–1880 MHz) • GSM1900 (1850–1990 MHz), • UMTS band II (1850–1990 MHz) • UMTS band I (1920–2170 MHz) • LTE FDD, B2 (1850–1990) • LTE FDD, B3 (1710–1880) • Meteorological services (1690–1700 MHz)
Band II	3.45–5.01	• 5G NR, n78 (3300–3800) MHz • 5G NR, n77 (3300–4200) MHz • WiMAX (3300–3800 MHz) • LTE TDD, B42 (3400–3600) • LTE TDD, B43 (3600–3800) • IEEE 802.11y (3650–3700 MHz)
Band III	5.19–6.07	• WLAN (5150–5350, 5725–5825 MHz) • ISM (5725–5825 MHz) • WiMAX (5250–5850 MHz) • IEEE 802.11a and other C-band applications, including satellite communications. • 5G Unlicensed band (5.2–5.7 GHz)
Band IV	6.09–7.06	• Satellites communications
	$\|S11\| \leq$ -10 dB	
Band	Bandwidth (GHz)	Applications
Band I	1.89–2.00	• UMTS band I (1920–2170 MHz) • 4G LTE FDD, B1 (1920–2170 MHz)
Band II	3.74–4.77	• 5 G (3200–3800 MHz) • C-band downlink Satellite communication (3700–4200 MHz) • IMT (3G/4G) (3400–4200, 4400–4900) MHz
Band III	5.28–5.63	• WiMAX (5250–5850 MHz) • IEEE 802.11a (5.47–5.725GHz) • 5G Unlicensed band (5.2–5.7GHz)
Band IV	6.24–6.46	• Satellites communications

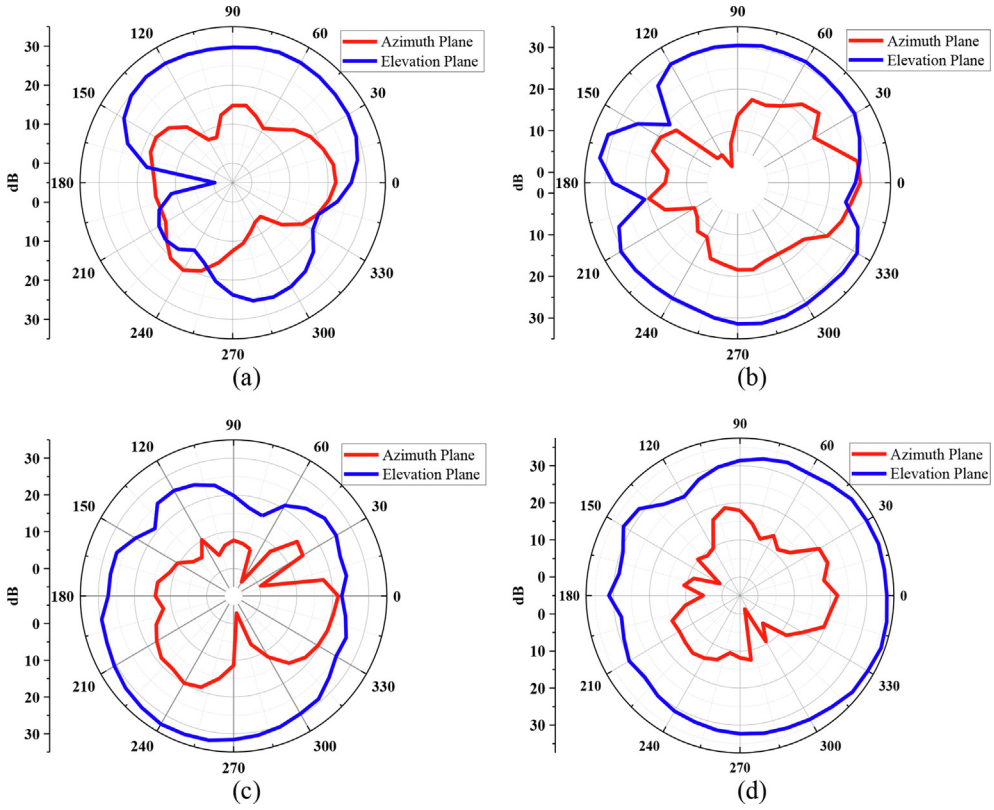

Figure 10. Measured 2D radiation patterns of the antenna at: (a)1.95 GHz, (b) 4.16 GHz, (c) 5.35 GHz, (d) 6.33 GHz.

Table 3. Simulated efficiency of the proposed antenna.

Simulated results	Resonant frequency			
	1.95 GHz	3.99 GHz	5.14 GHz	6.27 GHz
Radiated power (mW)	17.48	391.26	267.51	305.09
Accepted power (mW)	81.58	472.65	478.01	525.58
Incident power (mW)	1000	1000	1000	1000
Radiation efficiency (%)	21.43	82.78	55.96	58.05
Total efficiency (%)	1.75	39.13	26.75	30.51

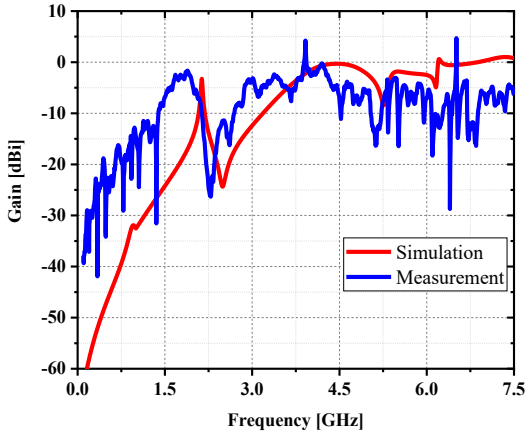

Figure 11. Simulated and measured gain of the proposed antenna.

A single band and monopole heart-shaped antenna is designed to operate at 3.345 GHz. Following the planar monopole antennas' design theory described in [43], the lower frequency for the heart-shaped geometry can be approximated as

$$f_r = \frac{7.2}{\sqrt{\varepsilon_{eff}}\left\{3.121a + \frac{1}{6.242\pi a}\left[7.142a^2 - \left(\frac{W_f}{2}\right)^2\right] + p\right\}} \quad (1)$$

where p is the gap between the radiator and the ground plane, W_f the width of the microstrip feedline, "a" the radius of the antenna's circular part, and ε_{eff} the effective permittivity of the structure given by

$$\varepsilon_{eff} = \frac{\varepsilon_r + 1}{2} + \frac{\varepsilon_r - 1}{2}\left[1 + 12\frac{h}{(3.414a)}\right]^{-0.5} \quad (2)$$

To create multiband characteristics, multiple resonant structures through slots are used. Two open-ended branches and a heart-shaped slot at the center of the radiating element are created to generate three resonant frequencies, as depicted in Figure 2. In the geometry, the corresponding resonant path lengths L_i (i = 1, 2, 3) are close to quarter-wavelength at their fundamental resonant frequencies and can be computed as follow:

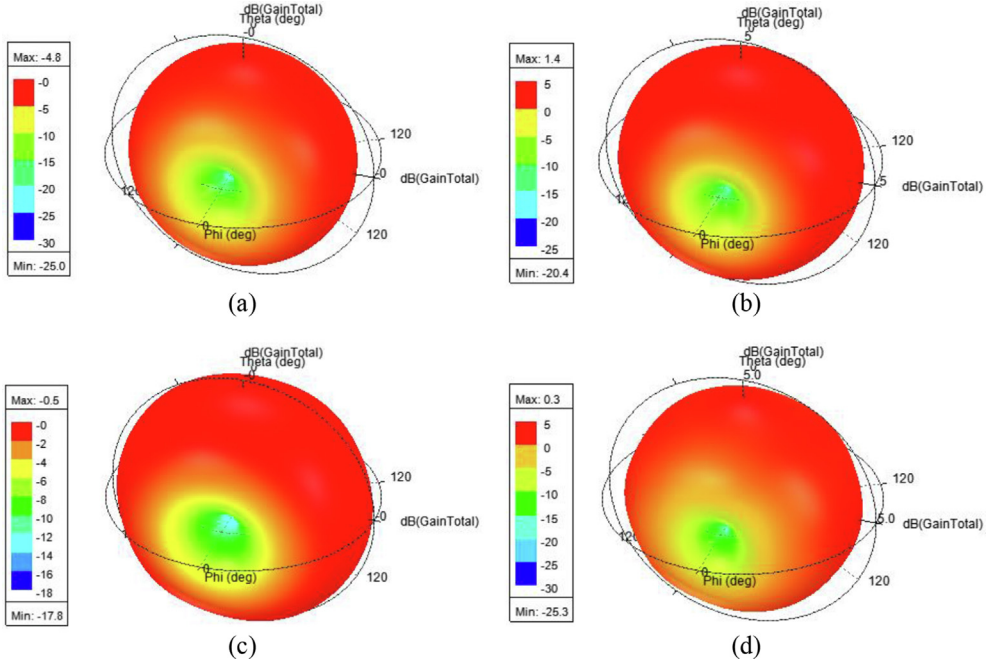

Figure 12. Simulated gain of the proposed antenna at: (a) 1.95 GHz, (b) 3.99 GHz, (c) 5.14 GHz, (d) 6.27 GHz.

$$f_{i_{(GHz)}} \approx \frac{75}{L_{i_{(mm)}}\sqrt{\varepsilon_{eff}}} \tag{3}$$

$$L_i = 10.283a_i, \quad i = 1,\ 2,\ 3 \tag{4}$$

This second step of the design procedure is experimentally tested through the fabrication and measurement of the triband antenna prototype presented in Figure 2. The measured results show that the triband resonates at 2.89 GHz, 3.73 GHz, and 6.73 GHz. The first to the thirds band's return loss is about -19.6 dB, -40.93 dB, and -21.58 dB, respectively.

Two metallic vias, and a parasitic conductor element has been added to the antenna design structure to achieve the proposed antenna's desired performance. This yielded in lowering the resonant frequency of the first band, generating a fourth band, and improving the return loss level, as shown in Figure 3. This made it possible for the proposed antenna to operate in GSM1800, GSM1900, and 5 GHz WLAN bands.

By reducing the dynamic range of the reflection coefficient plots presented in Figure 3, from -12 dB to 0, the following Figure 4 is obtained.

It is important to note that the shape of the parasitic conductor element placed at the bottom of the dielectric material influences the results. Three shapes with the same surface area of 32.64 mm^2 have been simulated to evaluate the parasitic conductor element's effect on the antenna performance. The circular shape has a radius of 3.22 mm, whereas the square shape's edges length is about 5.71 mm. The results are presented in Figure 5.

It can be observed that the proposed shape yields better results (in terms of matching level) as compared to the circular and square shapes.

From all the details presented above, the proposed antenna design methodology can be summarized as follows:

- Design of a monoband heart-shaped planar monopole antenna resonating at 3.345 GHz using Eqs. (1) and (2);
- Creation of multiband characteristic by making two open-ended heart-shaped branches through slits and a slot of identical shape, located at the center of the main radiating element. The Eqs. (2), (3), and (4) are employed for estimating and achieving the desired results;
- Insertion of a parasitic conducting element which is connected to the slitted patch by two metallic vias.

3. Simulated and measured results

Figure 6 illustrates the manufactured prototypes of the proposed quadband antenna. The top radiating element area is about 28.504 mm^2, placed on a 1.25 × 1.5 cm^2 insulator. The two metallic vias are identical and have a diameter of 100 μm. The ground plane's surface area is about 1.25 × 0.3 cm^2, whereas the parasitic conductor element at the bottom of the substrate has an active area of approximately 32.64 mm^2.

3.1. Antenna return loss

The simulated and measured return loss results are presented in Figure 7. The experimental and simulation results agree with some discrepancies observed at certain frequencies from the frequency response plots, but the graphs have the same trend.

As for Figure 3, Figure 7 is zoomed in by reducing the dynamic range and plotting the results from -12 dB to 0 (see Figure 8).

By considering all the frequency bands covered by the predefined limit for mobile terminal antennas ($|S_{11}| \leq$ -6 dB) [44, 45, 46, 47], the experimental frequency response results demonstrate that antenna exhibits a minimum bandwidth of 380 MHz at its lower band and can operate across the GSM, UMTS, LTE, 5G, WLAN, WiMAX, ISM, and C-band satellite communication bands.

When the reading reference is -10 dB, which is the most commonly used in microwave engineering, the proposed antenna can still cover several wireless applications such as UMTS, LTE, 5G, WLAN, WiMAX, and C-band applications. Table 2 summarizes the applications covered by the proposed antenna for $|S_{11}| \leq$ -6 dB and $|S_{11}| \leq$ -10 dB.

3.2. Voltage Standing Wave Ratio (VSWR)

Figure 9 displays the optimized quadband antenna's impedance matching in terms of Voltage Standing Wave Ratio (VSWR). Both simulated and measured results are presented. It can be observed that the proposed compact antenna meets the requirement of 2:1 VSWR with a maximum value of 1.674 across all the operating frequency bands. This good impedance matching results in less reflected power at the antenna feed point.

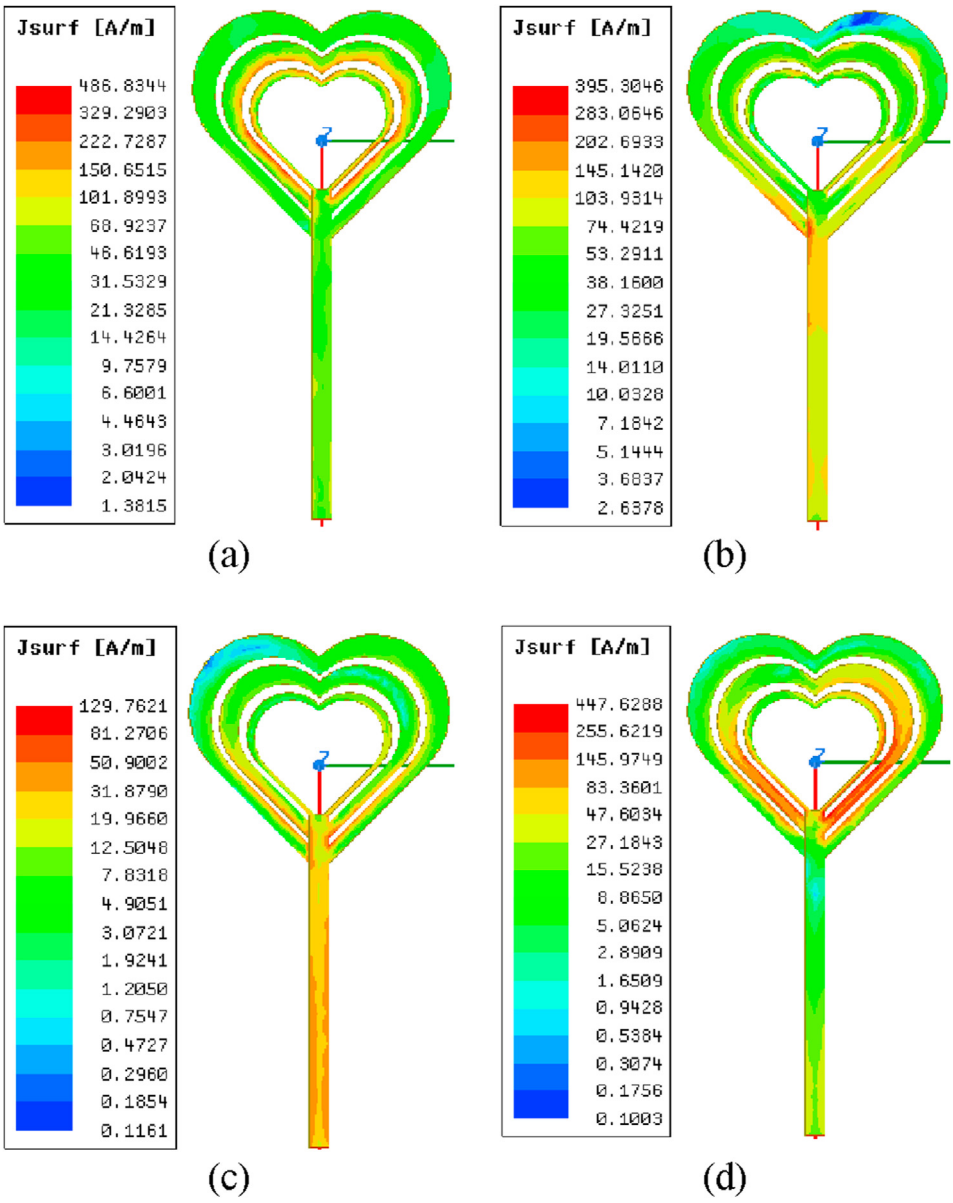

Figure 13. Surface current distribution of the proposed antenna at: (a) 1.95 GHz, (b) 3.99 GHz, (c) 5.14 GHz, (d) 6.27 GHz.

3.3. Antenna radiation pattern, efficiency, and gain

The far-field radiation patterns of the proposed QHPMA are illustrated in Figure 10. A nearly omnidirectional characteristic is observed in the Elevation plane at all the operating frequency bands, except for the first band, where the pattern is quasi-directional. Similarly, in the Azimuth plane, a quasi-bidirectional characteristic is observed on the second, third, and fourth bands. The first band exhibits an arbitrary shape radiation pattern.

The proposed antenna's simulated radiation efficiency is 21.43%, 82.78, 55.96%, and 58.05% at 1.95 GHz, 3.99 GHz, 5.14 GHz, and 6.27 GHz, respectively. The total efficiency includes the mismatch between the feedline/connector and the antenna given by [48].

$$\eta_T = \frac{P_{rad}}{P_s} = \eta_{rad}\left[1 - |\Gamma|^2\right] \tag{5}$$

where P_{rad} is the total radiated power by the antenna, P_s the total power supplied to the antenna, η_{rad} the antenna's radiation efficiency, and Γ is the reflection coefficient (the same as S_{11} or S_{22}). Based on the simulated results, the proposed antenna's radiation characteristics are summarized in Table 3 below.

Figure 11 illustrates the simulated and measured gains for the proposed quadband antenna, and the plots show the same trend. The experimental results demonstrate that the maximum gain within the desired frequency bands is about -1.65 dBi at 1.88 GHz, 4.23 dBi at 3.91 GHz, -3.03 dBi at 5.46 GHz, and 4.7 dBi at 6.51 GHz for the first, the second, the third, and the fourth band, respectively. Moreover, the gains at the respective resonant frequencies 1.95 GHz, 4.16 GHz, 5.35 GHz, and 6.33 GHz are -3.08 dBi, -0.96 dBi, -8.52 dBi, and -7.46 dBi, respectively.

All the gain results presented above have been computed using a reference (receiving) antenna and applying the *Two - Antenna Method* [49] based on the Friis' formula given by

$$G_t^{dBi} = S_{21}^{dB} + 32.5 + 20\log\left[f_{0_{(GHz)}}\right] + 20\log[d_{(m)}] - G_{ref}^{dBi} \tag{6}$$

where G_t and G_{ref} denote respectively the gain of the transmitting and receiving antennas, f_0 the operating frequency, the distance between

Table 4. Comparison of the proposed antenna with some other multiband antennas.

Ref.	Substrate	Size	Frequency band (GHz)	Applications	Gain	Radiation efficiency (%)	Proposed method	Operating bands
[2]	FR4 ($\varepsilon_r = 4.3$)	$0.285\lambda_0 \times 0.188\lambda_0 \times 0.004\lambda_0$	1.5–2.8 3.2–6	GSM, UMTS, LTE, Wi-Fi, WiMAX, lower UWB application	1.0–4.0 dBi	Not provided	Slots, slits, and DGS	Dual
[50]	Rogers RTDuroid5870 ($\varepsilon_r = 2.33$)	$0.115\lambda_0 \times 0.128\lambda_0 \times 0.005\lambda_0$	1.90–2.25 3.32–3.79 5.14–5.83 7.22–7.78	UMTS, WLAN, WiMAX, Downlink Satellite System	3.00–5.32 dBi 3.98–5.22 dBi 3.69–5.52 dBi 3.38–5.52 dBi	89	Slits, DGS, reconfigurable diodes	Quad
[51]	FR4 ($\varepsilon_r = 4.4$)	$0.238\lambda_0 \times 0.3291\lambda_0 \times 0.008\lambda_0$	1.43–1.6 1.94–2.1 2.4–2.57 3.45–3.6	GNSS, UMTS, WLAN, WiMAX	1.08 dBic 1.38 dBi 0.85 dBi 0.7 dBi	Not provided	Multiple branches technique, DGS, slits, and stub	Quad
[52]	FR4 ($\varepsilon_r = 4.4$)	$0.237\lambda_0 \times 0.142\lambda_0 \times 0.008\lambda_0$	1.42–2.08 3.49–4.13 5.23–7.53 8–9.87 10.7–20	GSM, WiMAX, WLAN, X-Band, Ku-Band	2.1–6.5 dBi	Not provided	Stubs and DGS	Penta
[53]	FR4 ($\varepsilon_r = 4.4$)	$0.271\lambda_0 \times 0.271\lambda_0 \times 0.009\lambda_0$	1.69–1.94 3.64–3.88	GSM, WiMAX	≈ 2–7 dB	82–86	Circular ring and U-shaped slots, and DGS	Dual
[54]	Rogers RO4533 ($\varepsilon_r = 3.45$)	$0.355\lambda_0 \times 0.027\lambda_0 \times 0.003\lambda_0$	1.61–2.21	GSS phones (uplink), AWS, GSM, WCDMA/IMT-2000, UMTS, LTE bands.	2.45 dBi	34–48	Slots and DGS	Single
[55]	FR4 ($\varepsilon_r = 4.5$)	$0.084\lambda_0 \times 0.064\lambda_0 \times 0.003\lambda_0$	0.6–0.64 2.67–3.40 3.61–3.67	LTE, Bluetooth, WiMAX	3.00–3.69 dBi	Not provided	Multiple branches technique, metamaterial, and DGS	Dual
This work	FR4 ($\varepsilon_r = 4.2$)	$0.095\lambda_0 \times 0.079\lambda_0 \times 0.006\lambda_0$	1.89–2.00 3.74–4.77 5.28–5.63 6.24–6.46	GSM, UMTS, LTE, 5G, WLAN, WiMAX, ISM, C-band satellite communications	-7.46 – 4.7 dBi	21.43–82.78	Multiple branches technique, DGS, shorting pins (metallic via holes), and parasitic element	Quad

both antennas, and S_{21} the transmission coefficient between both antennas.

The simulated gain is depicted in Figure 12, where it can be observed a gain of -4.8 dB, 1.4 dB, -0.5 dB, and 0.3 dB at 1.95 GHz, 3.99 GHz, 5.14 GHz, and 6.27 GHz, respectively.

The peak of the simulated gain is achieved at 3.99 GHz, with of value of 1.4 dB.

3.4. Current distribution

The surface current distribution of the proposed QHPMA at various resonant frequencies is presented in Figure 13. This reveals parts of the antenna that play a crucial role at the given frequency.

The results are plotted at 1.95 GHz, 3.99 GHz, 5.14 GHz, and 6.27 GHz. It can be observed that the current is higher at around the second slit with a maximum intensity of 486.8 A/m for the lower band. In contrast, for the second and third band, the surface current is concentrated around the feedline, the first open-ended branch, and the first slit. The maximum current is about 395.3 A/m and 129.7 A/m at the second and the third resonant frequencies. At 6.27 GHz, the surface current is more vivid in the upper band around the second open-ended branch and around the microstrip feed line with a maximum of 447.62 A/m.

The proposed QHPMA is compared to other existing single layer multiband antennas found in literature, as presented in Table 4.

The data provided in Table 4 illustrate that the available antenna designs have either large size or cannot cover all the cellular network technology standards. Moreover, the proposed quadband antenna discussed in this paper gives better performance than the references in terms of size, multiband operation, lightweight, low profile, and compactness. With the overall physical size of $15 \times 12.5 \times 1$ mm^3, the proposed antenna is the smallest single-layer antenna operating in the GSM frequency band. Its characteristics, as mentioned above, make it suitable for integration into portable devices and use in multiband wireless systems.

4. Conclusion

In this paper, an ultra-miniaturized quadband heart-shaped monopole antenna (QHPMA) has been presented, analyzed and discussed. The desired antenna performances have been achieved due to the slits, the metallic vias, and the partial ground plane technique without an additional matching circuit. The agreement between the simulated and measured results validated the QHPMA design technology and its feasibility of implementation. The measured results demonstrate that the QHPMA achieves a minimum impedance bandwidth ($|S11| \leq$ -10 dB) of 110 MHz and exhibits a peak gain of 4.7 dBi at 6.51 GHz. With an overall size of $0.095\lambda0 \times 0.079\lambda0 \times 0.006\lambda0$ at 1.89 GHz, a radiation efficiency ranging from 21.43% to 82.78 % has been found from simulation data. The designed QHPMA has its application in all the generations of mobile networks (2G, 3G, 4G, and 5G) in addition to other modern wireless applications, including WLAN, WiMAX, ISM, meteorological services, and C-band satellite communications. Its stunning performance and features make it an up-and-coming candidate in the smartphones and mobile terminal industries.

Declarations

Author contribution statement

Pierre Moukala Mpele: Conceived and designed the experiments; Performed the experiments; Analyzed and interpreted the data; Contributed reagents, materials, analysis tools or data; Wrote the paper.

Franck Moukanda Mbango: Performed the experiments; Analyzed and interpreted the data; Contributed reagents, materials, analysis tools or data.

Dominic B.O Konditi: Analyzed and interpreted the data; Contributed reagents, materials, analysis tools or data.

Fabien Ndagijimana: Performed the experiments.

Funding statement

This work was supported by the African Union Commission through the Pan African University Institute for Basic Sciences Technology and Innovation (PAUSTI).

Data availability statement

No data was used for the research described in the article.

Declaration of interests statement

The authors declare no conflict of interest.

Additional information

No additional information is available for this paper.

Acknowledgements

Grateful acknowledgment is made to Pheline Laboratory for great guidance during the prototype's validation process.

References

[1] J. Volakis, Antenna Engineering Handbook, fourth ed., McGraw Hill Wiley Wiley, 2007.
[2] R. Roshan, S. Prajapati, H. Tiwari, G. Govind, A dual wideband monopole antenna for GSM/UMTS/LTE/WiFi/and lower UWB application, in: 2018 3rd Int. Conf. Microw. Photonics, ICMAP 2018, vol. 2018-Janua,no. Icmap, 2018, pp. 1–2.
[3] M. Alibakhshikenari, M. Khalily, B.S. Virdee, C.H. See, R.A. Abd-Alhameed, E. Limiti, Mutual-coupling isolation using embedded metamaterial em bandgap decoupling slab for densely packed array antennas, IEEE Access. 7 (2019) 51827–51840.
[4] R. Zhi, M. Han, J. Bai, W. Wu, G. Liu, Miniature multiband antenna for WLAN and X-Band satellite communication applications, Prog. Electromagn. Res. Lett. 75 (April) (2018) 13–18.
[5] D. Upadhyay, R.P. Dwivedi, Antenna miniaturization techniques for wireless applications, in: IFIP International Conference on Wireless and Optical Communications Networks, WOCN, 2014, pp. 1–4.
[6] I. Aggarwal, M.R. Tripathy, S. Pandey, A novel design of fractal antenna: effect of different dielectric substrate materials, in: Recent Trends in Materials and Devices, 2017, pp. 521–526.
[7] S. Ullah, C. Ruan, M.S. Sadiq, T.U. Haq, W. He, High efficient and ultra wide band monopole antenna for microwave imaging and communication applications, Sensors 20 (1) (Dec. 2019) 115.
[8] S. Wang, F. Kong, K. Li, L. Du, A planar triple-band monopole antenna loaded with an arc-shaped defected ground plane for WLAN/WiMAX applications, Int. J. Microw. Wirel. Technol. (2020).
[9] M. Karthikeyan, R. Sitharthan, T. Ali, B. Roy, Compact multiband CPW fed monopole antenna with square ring and T-shaped strips, Microw. Opt. Technol. Lett. 62 (2) (2020) 926–932.
[10] Z. Ding, H. Wang, S. Tao, D. Zhang, C. Ma, Y. Zhong, A novel broadband monopole antenna with T-slot, CB-CPW, parasitic stripe and heart-shaped slice for 5G applications, Sensors 20 (24) (Dec. 2020) 7002.
[11] A.Z. Manouare, S. Ibnyaich, A. EL Idrissi, A. Ghammaz, N.A. Touhami, "A compact dual-band CPW-fed planar monopole antenna for 2.62–2.73 GHz frequency band, WiMAX and WLAN applications, J. Microwaves, Optoelectron. Electromagn. Appl. 16 (2) (Apr. 2017) 564–576.
[12] Y. Li, Z. Zhang, M.F. Iskander, Antenna miniaturization in mobile communication systems, in: The World of Applied Electromagnetics, Springer International Publishing, Cham, 2018, pp. 205–226.
[13] M.S. Sharawi, M.U. Khan, R. Mittra, Microstrip patch antenna miniaturisation techniques: a review, IET Microw. Antennas Propag. 9 (9) (Jun. 2015) 913–922.
[14] M. Fallahpour, R. Zoughi, Antenna miniaturization techniques: a review of topology- and material-based methods, IEEE Antenn. Propag. Mag. 60 (1) (Feb. 2018) 38–50.
[15] M. Tarbouch, A. Elamri, H. Terchoune, Contribution to the miniaturization of antennas: state of the art, Trans. Networks Commun. 4 (5) (2016).
[16] B. Roy, A. Bhattacharya, R. Karmakar, S.K. Chowdhury, A.K. Bhattacharjee, A compact wideband monopole antenna designed for wireless applications, in: 2016 Loughborough Antennas and Propagation Conference, LAPC 2016, 2017, pp. 5–8.
[17] O. Oulhaj, N.A. Touhami, M. Aghoutane, A. Tazon, A miniature microstrip patch antenna array with defected ground structure, Int. J. Microw. Opt. Technol. 11 (1) (2016) 32–39.
[18] F.A. Lalitha Bhavani Konkyana, B. Alapati Sudhakar, A review on microstrip antennas with defected ground structure techniques for ultra-wideband applications, in: Proc. 2019 IEEE Int. Conf. Commun. Signal Process. ICCSP 2019, 2019, pp. 930–934.
[19] P. Moukala Mpele, F. Moukanda Mbango, D.B. Onyango Konditi, A small dual band (28/38 GHz) elliptical antenna for 5G applications with DGS, Int. J. Sci. Technol. Res. 8 (10) (2019) 353–357.
[20] M. Alibakhshi-Kenari, M. Naser-Moghadasi, Novel UWB miniaturized integrated antenna based on CRLH metamaterial transmission lines, AEU - Int. J. Electron. Commun. 69 (8) (2015) 1143–1149.
[21] M. Mehrparvar, F.H. Kashani, Microstrip Antenna Miniaturization Using Metamaterial Structures, 2012, pp. 1243–1246.
[22] R. Porath, Theory of miniaturized shorting-post microstrip, IEEE Trans. Antenn. Propag. 48 (1) (2000) 41–47.
[23] K.F. Lee, K.F. Tong, Microstrip patch antennasbasic characteristics and some recent advances, Proc. IEEE 100 (7) (2012) 2169–2180.
[24] D.K. Karmokar, S.L. Chen, Slot antenna miniaturization by loading dumbbell-shaped slots and strips, square-shaped loops, and shorting vias, Microw. Opt. Technol. Lett. (March 2019) (2020) 3–6.
[25] U. Shameem, M. Ur-Rehman, Q.H. Abbasi, K. Qaraqe, "A low profile penta-band antenna for portable devices," *2016*, Int. Work. Antenna Technol. iWAT 9781509002 (June) (2016) 174–177.
[26] P.K. Rao, K.M.J. Singh, A circular shaped microstrip patch antenna for bluetooth/wi-fi/UWB/X-band Applications, in: 2018 International Conference on Power Energy, Environment and Intelligent Control (PEEIC), 2018, pp. 638–641.
[27] Y.Z.H. Jin, C.M. Li, A compact dual-wideband monopole antenna with parasitic patch for 2G/3G/LTE/WLAN/WiMAX applications, in: Conference: 2017 IEEE 5th International Symposium on Electromagnetic Compatibility (EMC-Beijing), 2017, pp. 7–10.
[28] Z. Yu, J. Yu, X. Ran, C. Zhu, A novel Koch and Sierpinski combined fractal antenna for 2G/3G/4G/5G/WLAN/navigation applications, Microw. Opt. Technol. Lett. 59 (9) (2017) 2147–2155.
[29] T. Ali, K.D. Prasad, R.C. Biradar, A miniaturized slotted multiband antenna for wireless applications, J. Comput. Electron. 17 (3) (Sep. 2018) 1056–1070.
[30] A.K. Skrivervik, J.F. Zürcher, O. Staub, J.R. Mosig, PCS antenna design: the challenge of miniaturization, IEEE Antenn. Propag. Mag. 43 (4) (2001) 12–27.
[31] J. Zhou, W. Terminal, D. Team, Developing reliable antennas for smartphones, ANSYS Advant. IX (1) (2015) 44–46.
[32] M. Gadag, S. Joshi, N. Gadag, Performance comparison of rectangular and circular micro-strip antenna at 2.4 GHz for wireless applications using IE3D, in: Intelligent Communication and Computational Technologies, 2018, pp. 181–190.
[33] S.S. Chakravarthy, N. Sarveshwaran, S. Sriharini, M. Shanmugapriya, Comparative study on different feeding techniques of rectangular patch antenna, in: 2016 Thirteenth International Conference on Wireless and Optical Communications Networks (WOCN), Jul. 2016, pp. 1–6.
[34] P.K. Bharti, G.K. Pandey, H.S. Singh, M.K. Meshram, A compact multiband planar monopole antenna for slim mobile handset applications, Prog. Electromagn. Res. B 61 (1) (2015) 31–42.
[35] J.Y. Deng, J. Yao, L.X. Guo, Compact multiband antenna for mobile terminal applications, Microw. Opt. Technol. Lett. 60 (7) (2018) 1691–1696.
[36] J.Y. Deng, S.Y. Liu, D. quan Sun, L.X. Guo, S. Bin Xue, Multiband antenna for mobile terminals, Int. J. RF Microw. Comput. Eng. 29 (11) (2019) 1–7.
[37] J. Pang, M. Zhu, G. Yu, H. Zhou, A nona-band narrow-frame antenna with a defected ground structure for mobile phone applications, Microw. Opt. Technol. Lett. 62 (1) (2020) 498–506.
[38] Y. Liu, W. Cui, Y. Jia, A. Ren, Hepta-band metal-frame antenna for LTE/WWAN full-screen smartphone, IEEE Antenn. Wireless Propag. Lett. 19 (7) (2020) 1241–1245.
[39] L. Belrhiti, F. Riouch, A. Tribak, J. Terhzaz, A.M. Sanchez, Internal compact printed loop antenna for WWAN/WLAN/ISM/LTE smartphone applications, Int. J. Microw. Wirel. Technol. 9 (10) (Dec. 2017) 1961–1973.
[40] S. Risco, J. Anguera, A. Andújar, A. Pérez, C. Puente, Coupled monopole antenna design for multiband handset devices, Microw. Opt. Technol. Lett. 52 (2) (Feb. 2010) 359–364.
[41] M.G. Lountala, F. Moukanda Mbango, F. Ndagijimana, D. Lilonga-Boyenga, Movable short-circuit technique to extract the relative permittivity of materials from a coaxial cell, J. Meas. Eng. 7 (4) (Dec. 2019) 183–194.
[42] F.M. Mbango, J.E. Delfort M'pemba, F. Ndagijimana, B. M'passi-Mabiala, Use of two open-terminated coaxial transmission-lines technique to extract the material relative intrinsic parameters, IEEE Access. 8 (2020) 138682–138689.
[43] G. Kumar, K.P. Ray, Broadband Microstrip Antennas, Artech House, 2003.
[44] Y. Xu, Y.W. Liang, H.M. Zhou, "Small-size reconfigurable antenna for WWAN/LTE/GNSS smartphone applications, IET Microw. Antenn. Propag. 11 (6) (2017) 923–928.
[45] H. Jian-rong, L. Jiu-sheng, W. Di, A small planar antenna for 4G mobile phone application, Int. J. Antenn. Propag. 2016 (2016) 1–7.

[46] M. Yang, Y. Sun, F. Li, A compact wideband printed antenna for 4G/5G/WLAN wireless applications, Int. J. Antenn. Propag. 2019 (Sep. 2019) 1–9.
[47] C. Luxey, A. Cihangir, Antennas in handheld devices, in: Z.N. Chen, D. Liu, H. Nakano, X. Qing, T. Zwick (Eds.), Handbook of Antenna Technologies, 1–4, Springer Singapore, Singapore, 2016, pp. 3077–3138.
[48] Y. Huang, Radiation efficiency measurements of small antennas, in: Z.N. Chen (Ed.), Handbook of Antenna Technologies, no. 2, Springer Singapore, Singapore, 2015, pp. 1–21.
[49] C.A. Balanis, Antenna Theory : Analysis and Design, fourth ed., Wiley, 2016.
[50] N. Kumar, P. Kumar, M. Sharma, Reconfigurable minitaurized multiband Antennas for UMTS, WiMAX, WLAN downlink satellite system wireless applications, in: 2019 1st Int. Conf. Signal Process. VLSI Commun. Eng. ICSPVCE 2019, 1, 2019, pp. 4–8.
[51] R.S. Brar, K. Saurav, D. Sarkar, K.V. Srivastava, A quad-band dual-polarized monopole antenna for GNSS/UMTS/WLAN/WiMAX applications, Microw. Opt. Technol. Lett. 60 (3) (2018) 538–545.
[52] B. Bag, P. Biswas, S. De, S. Biswas, P.P. Sarkar, A wide multi-band monopole antenna for GSM/WiMAX/WLAN/X-Band/Ku-Band Applications, Wirel. Pers. Commun. 111 (1) (2020) 411–427.
[53] S.P. Gangwar, K. Gangwar, A. Kumar, Dual band modified circular ring shaped slot antenna for GSM and WiMAX applications, Microw. Opt. Technol. Lett. 61 (12) (2019) 2752–2759.
[54] A. Affandi, R. Azim, M.M. Alam, M.T. Islam, A low-profile wideband Antenna for WWAN/LTE applications, Electronics 9 (3) (Feb. 2020) 393.
[55] M.M. Hasan, M.R.I. Faruque, M.T. Islam, Dual band metamaterial antenna for LTE/bluetooth/WiMAX system, Sci. Rep. 8 (1) (2018) 1–17.